5-14-2011

Characterization of esterase activity from the bacteria, Francisella tularensis, the causative agent of tularemia

Leigh Anna Weston
Butler University

BUTLER UNIVERSITY HONORS PROGRAM

Honors Thesis Certification

Please type all information in this section:

Applicant Leigh Anna Weston
(Name as it is to appear on diploma)

Thesis title Characterization of esterase activity from the bacteria, *Francisella tularensis*, the causative agent of tularemia

Intended date of commencement May 14, 2011

Read, approved, and signed by:

Thesis adviser(s) R. Jeremy Johnson 4/22/11
Date

Reader(s) Geoffrey C. Hoops 4/22/2011
Date

Date

Certified by Judith Harper Morrel 6/2/2011
Director, Honors Program Date

For Honors Program use:

Level of Honors conferred: University Magna Cum Laude

Departmental

Characterization of esterase activity from the bacteria, *Francisella tularensis,* the causative agent of tularemia

A Thesis

Presented to the Department of Chemistry

College of Liberal Arts and Sciences

and

The Honors Program

of

Butler University

In Partial Fulfillment of the Requirements for Graduation Honors

Leigh Anna Weston

April 2011

TABLE OF CONTENTS

TABLE OF FIGURES AND TABLES

Abstract

Francisella tularensis is the bacteria responsible for causing the disease tularemia and is listed as one of the top three-biowarfare agents. Among the proteins essential to the virulence and infectivity of *F. tularensis* are multiple esterases, which are enzymes that break down various ester, thioester, and amide bonds. In this project, the catalytic activity, substrate specificity, and structure of a putative esterase from *F. tularensis* was studied. Latent fluorophores based on the molecule, fluorescein, were unmasked by the enzymatic activity of the esterase and the increase in fluorescence was measured over time to determine how well the esterase recognized different substrates. The esterase FTT258C from *F. tularensis* activated a variety of simple latent fluorophore substrates with catalytic efficiencies ranging from 5075 $M^{-1}s^{-1}$ for a simple propyl ester to 294.8 $M^{-1}s^{-1}$ for a tertiary ester. These simple substrates were recognized by the esterase with K_M values ranging from 0.54 to 21.4 μM, and sterically occluded substrates had significantly reduced kinetic turnover (k_{cat}) compared to the simplest substrates. In addition to the wild type esterase, the kinetic activity of five different variants of the esterase with single amino acid mutations were characterized against two latent fluorophore substrates to determine more information about the binding pocket of the esterase. The kinetic activity of each of the variants decreased significantly from the wild-type enzyme activity and indicated that the binding pocket is fairly invariant to substitution. Activity, 3D structure, and primary structure comparisons suggest that this esterase belongs to the carboxylesterase family. Although little is known about the specific biological role of FTT0258C and other carboxylesterases from its family, the promiscuity of its enzymatic

activity could be used to develop potential drug models that utilize the unique action of the enzyme.

Background and Significance

Francisella tularensis, the Causative Agent of Tularemia

Francisella tularensis is the bacteria responsible for causing the disease, tularemia, which is commonly known as rabbit fever (Beckstrom-Sternberg). This infection is most commonly spread through bites from rodents or infected insects, but it can also be contracted from contaminated food and water (Su). While this disease is uncommon in the general population, it has been classified as a potential weapon of bioterrorism. The extreme virulence and relatively high mortality rate of the disease combined with its ability to be spread through the use of an aerosol make tularemia a prime candidate for biological warfare (Su). Several common antibiotics are currently administered to treat tularemia including streptomycin and gentamicin (Pohanka). These common treatments, however, run the risk of selecting for disease resistance bacteria because they do not specifically target the bacteria's mechanism for infection.

The entire list of molecular components, such as genes and proteins, required for *F. tularensis'* virulence have been determined using organism-wide selection systems (Weiss). Amongst the list of factors causing virulence are many commonly known factors including the pathogenicity island, which are genes known to infect the host immune system (Weiss). Other classes of proteins essential to infection included an esterase, a common type of enzyme used to break-down cellular byproducts which was identified only by its genomic annotation (FTT0941c). Another esterase from *F. tularensis* that likely has similar function to FTT0941c is the esterase, FTT0258C. The function and activity of the esterase, FTT0258C, was the primary focus of this research (Weiss).

Enzymes

Enzymes, such as the esterase (FTT0258C) from *F. tularensis,* are common proteins with many functions including increasing the speed of a chemical reaction and rearranging chemical bonds (Nelson). The presence of an enzyme can increase the speed of slow chemical reactions and give the cell precise temporal and spatial control of a chemical reaction. Enzymes bind to specific chemicals known as substrates with which they perform their chemical reaction.

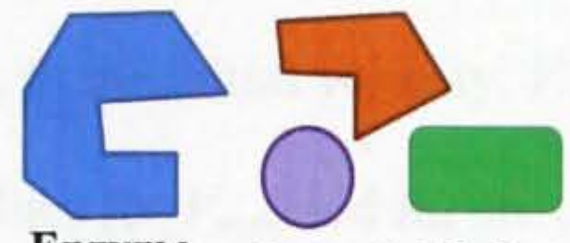

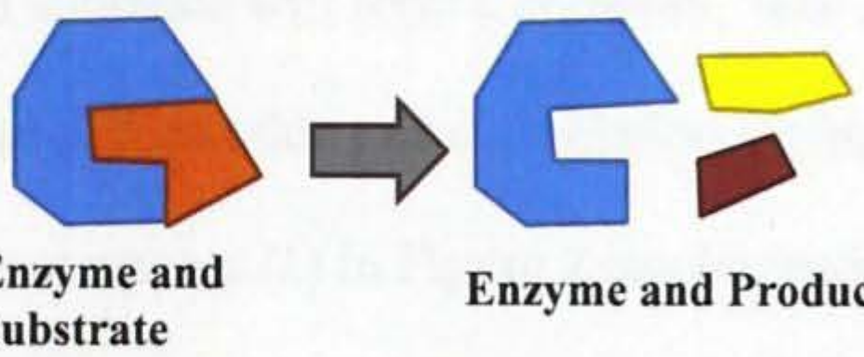

Figure 2: Schematic diagram of enzyme-substrate activity. Out of the three potential substrates, the one with the best fit will react with the enzyme.

The enzyme-substrate activity can be described in a manner similar to puzzle pieces fitting together as seen in Figure 1. Each enzyme has a characteristic three-dimensional shape that precisely matches the shape of its substrate. A small change to the overall structure of the enzyme or substrate can cause the pieces not to fit and the chemical reaction will no longer occur. An enzyme's ability to bind to a particular substrate is determined by the structure of the enzyme and the substrate, and the substrate specificity of an enzyme determines its biological function.

$$E + S \underset{k_{-1}}{\overset{k_1}{\rightleftharpoons}} ES \xrightarrow{k_2} E + P$$

Figure 1: Basic enzyme reaction. In this reaction, an enzyme, E, and substrate, S, form an enzyme-substrate complex, ES. The enzyme then converts the substrate into the desired product P. This basic enzyme reaction helps explain the Michaelis-Menten equation (Nelson)

The characteristics of substrate specificity and speed of catalysis can be quantified and related using the Michaelis-

Menten equation: $V_o = \frac{V_{max}\, x\, [Substrate]}{K_m + [Substrate]}$ (Equation 1). The Michaelis-Menten equation relates the maximum velocity of the enzymatic reaction, V_{max}, and equilibrium constant, K_m, to the initial velocity, V_o, and substrate concentration of an enzyme-substrate reaction. Values for V_{max} and K_m are constant for a specific enzyme concentration with a specific substrate. The Michaelis-Menten equation makes the basic assumptions that an enzyme and substrate will form a complex, "ES", and the concentration of "ES" achieves a steady state of formation and dissociation during the reaction (Figure 2) (Nelson). The kinetic rate constants (k) in Figure 2 can be rearranged to give the quantitative equilibrium constant, K_m, which can be related to the binding affinity between an enzyme and substrate.

The V_{max} value can be used along with the total enzyme concentration of a reaction to determine the turnover number, k_{cat}, for an enzyme-substrate reaction. The k_{cat} value is a measure of how quickly the enzyme is able to convert substrate into product at saturating substrate concentrations. The efficiency of an enzyme to bind substrate and produce product is quantified by the value, k_{cat}/K_M. A large value for this constant indicates an efficient enzyme reaction. In order to obtain values for V_{max} and K_m, the initial velocity of a reaction must be measured at a range of substrate concentrations (Nelson). The initial velocities of the reactions can be determined through enzyme reactions with latent fluorophore substrates, such as those used in this investigation.

An example of an enzyme is the serine protease, chymotrypsin, which is a

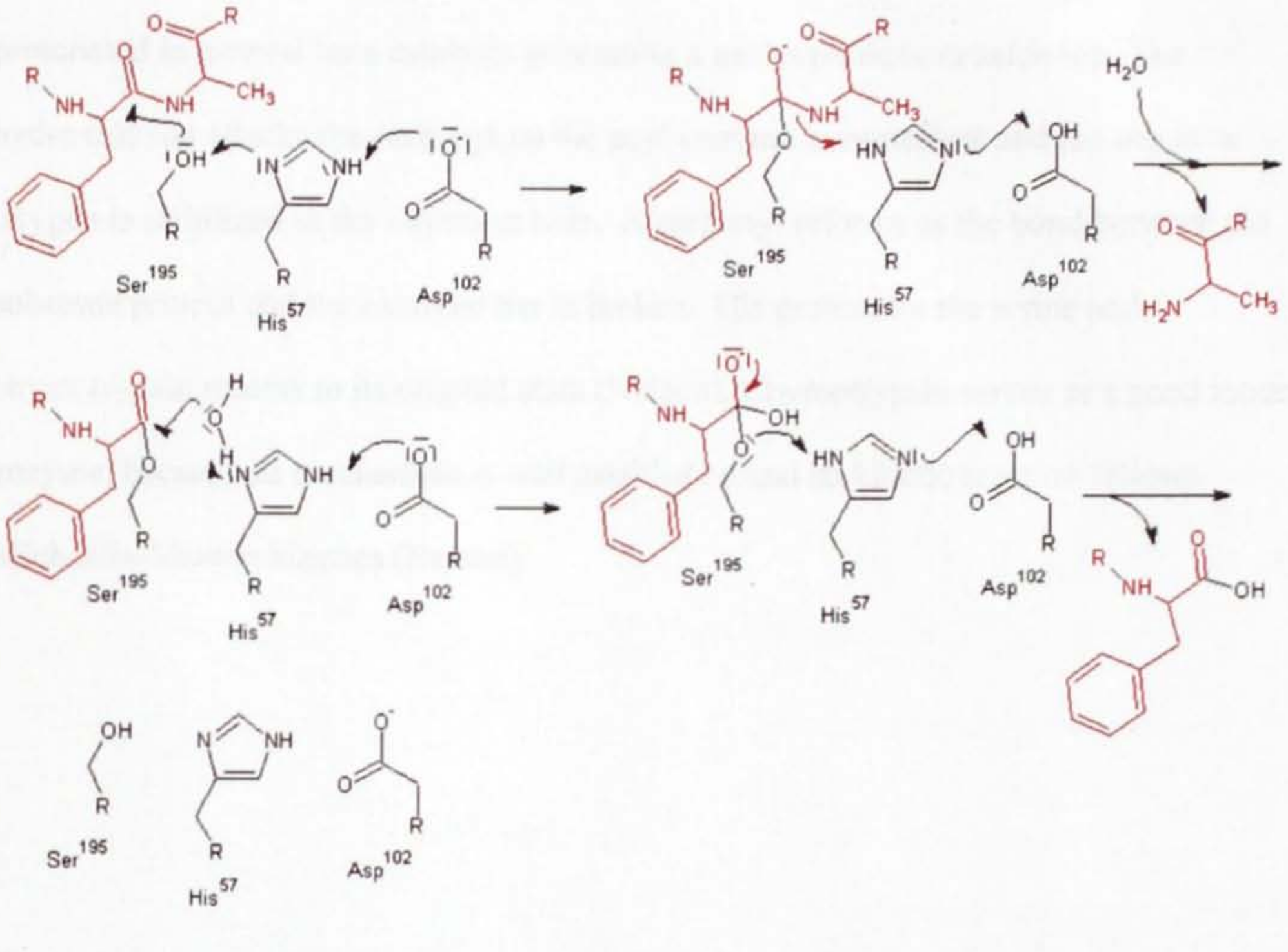

Figure 3: Mechanism of catalysis for the serine protease, chymotrypsin. (Plasser) The catalytic triad consists of Ser195, His57, and Asp102 with Ser195 being the catalytic residue. (Nelson)

common model enzyme used in biochemistry textbooks. Chymotrypsin catalyzes the cleavage of peptide bonds adjacent to tryptophan, phenylalanine, and tyrosine amino acid residues through acylation and subsequent deacylaction of a catalytic serine residue (Nelson). As seen in Figure 3, chymotrypsin uses a catalytic triad of residues featuring a serine, histidine, and an aspartate. In this mechanism, the catalytic serine residue, Ser 195, is de-protonated by His 57. The de-protonated Ser then acts as a nucelophile and attacks the carbonyl of the substrate protein peptide bond. The oxyanion hole of chymotrypsin stabilizes the resulting negative oxygen atom through hydrogen bonding. The oxygen of the tertiary intermediate then collapses to reform the carbonyl and the

peptide bond of the substrate protein is broken. This leaves the serine still bonded to part of the substrate protein as an acyl-enzyme intermediate. A water molecule is then de-protonated in general base catalysis generating a nucleophilic hydroxide ion. The hydroxide ion attacks the carbonyl on the acyl-enzyme intermediate and the negative oxygen is stabilized in the oxyanion hole. A carbonyl reforms as the bond between the substrate protein and the catalytic Ser is broken. His protonates the serine and, chymotrypsin returns to its original state (Nelson). Chymotrypsin serves as a good model enzyme, because its mechanism is well established and its kinetic reaction follows Michaelis-Menten kinetics (Nelson).

Esterases

An esterase is an enzyme with specified function for cleaving ester bonds. Although esterases primarily catalyze hydrolysis of ester bonds, the enzymes can also aid in the hydrolysis of thioester and amide bonds as seen in Figure 4 (Holmquist). Humans and bacteria have many different natural esterases whose biological roles, include triacylglycerol hydrolysis and xenobiotic detoxification and are utilized for a variety of functions including bioimaging and drug therapy (Lavis). Esterases also share a few other common characteristics, including their catalytic mechanism and overall structure.

Figure 4: Common hydrolysis reactions catalyzed by esterases. The top reaction, ester hydrolysis, is the reaction that is used to characterize the activity of FTT0258C from *F. tularensis.* (Holmquist)

For their catalytic mechanism, esterases utilize a conserved serine, histidine, and an aspartate residue, known as the catalytic triad, to perform ester bond hydrolysis (Pesaresi 2005 "Crystalization"). Their catalytic mechanism is identical to that of chymotrypsin, which is featured in Figure 3, except that the hydrolyzed bond is an ester instead of an amide. Important to this investigation is that a specific nucleophilic serine residue is deprotonated by the histidine and then acts as a nucleophile to attack the ester carbonyl (Pesaresi 2005 "Crystalization").

Carboxylesterases and Human Acylprotein Thioesterase 1 (ATP1)

One subclassification of esterases is the superfamily of serine carboxylesterases (EC 3.1.1.) that catalyze the hydrolysis of carboxylic acid ester bonds with short carbon chains (Pesaresi 2005 "Crystallization"). Interestingly, studies have shown that carboxylesterases have broad substrate specificity, suggesting the necessary evolution of the enzyme to be able to react with a large range of carbon sources (Pesaresi 2005 "Isolation"). Due to the promiscuous nature of these enzymes, specific physiological functions have not been precisely identified (Pesaresi 2010). Structural, genetic, and enzymatic activity studies of two carboxylesterases from *Pseudomonas aeruginosa* and *Pseudomonas fluorescens* were conducted to determine the probable function of these esterases *in vivo* (Pesaresi 2010 and Kim). The studies used to characterize these two carboxylesterases included structure determination by crystallography, thermal stability measurements, and kinetic activity determination with absorbent substrates with varying carbon chain lengths (Pesaresi 2010 and Kim). These carboxylesterases from *Pseudomonas* show significant sequence similarity to the esterase, FTT0258C, which was the enzyme investigated in this study. (Pesaresi 2010, 2005, 2005 and Kim).

While little is known about the specific physiological role of this family of bacterial carboxylesterases, these bacterial esterases have high sequence and structural similarity to human APT1 (Pesaresi 2010 and Kim). Substrate specificity of APT1 varies slightly among organisms, but in general APT1 is a lipase involved in the deacylation of post-translationally modified proteins (Zeidman). Certain proteins undergo a post-translational modification where a fatty acid chain is added to a cysteine residue through a thioester bond (Zeidman). The process of adding a fatty acid chain to a protein is

commonly referred to as S-acylation. Problems with the regulation of acylation and deacylation can cause a number of human diseases including Huntington's disease, a neurodegenerative disease (Zeidman). APT1 has a substrate preference for longer fatty acids, and more specifically palmitoyl acid (Zeidman). However, it is unknown if the bacterial carboxylesterases and the esterase from *F. tularensis* are utilized in a similar fashion as APT1 for the deacylation of proteins (Zeidman).

Fluorescence and Latent Fluorophores

Determination of an enzyme's kinetic activity can be completed through a variety of methods. One common method for determining the kinetic activity of esterases uses UV absorbent molecules with short acyl chains as esterase substrates (Pesaresi). The common esterase substrate, p-nitrophenyl acetate, is initially non UV absorbent, but upon ester hydrolysis, the product rearranges to the highly UV absorbent p-nitrophenyl (Figure 5). Beer's law:$A = \varepsilon bc$ (Equation 2) is then used to calculate the concentration of UV active substrate by relating the absorbance (A) of light at 410 nm to the concentration (c) by using the extinction coefficient (ε) for that substrate.

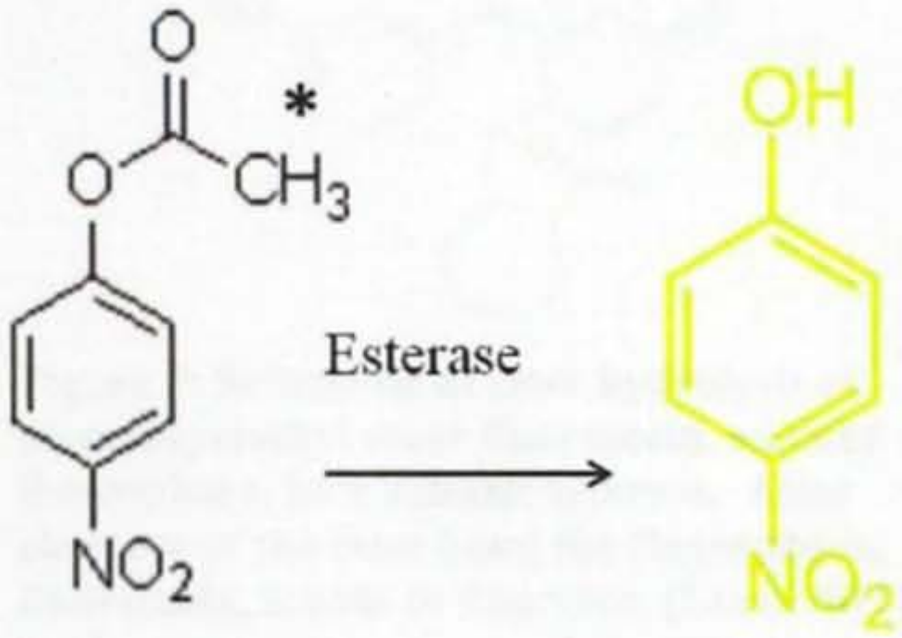

Figure 4: Esterase catalyzed hydrolysis of p-nitrophenyl acetate. These substrates can have various carbon chain lengths at the "*" position.

While p-nitrophenyl substrates have been useful for esterase characterization, absorbance measurements are not as sensitive as fluorescent signals and the chemical diversity of the substrates is limited (Pesaresi).

A similar method to characterize esterase activity has been developed using "latent" fluorophores. When a standard fluorophore, such as fluorescein, is exposed to a certain wavelength of light, it will absorb that light and subsequently emit light at a different wavelength. The phenomenon of giving off light is fluorescence (Lavis 2008). Latent fluorophores are fluorophores whose fluorescent activity that has been masked by the addition of new chemical groups. These chemical blocking groups can then be removed by an enzyme under the desired conditions (Figure 6). The latent fluorophores

being used for this study are seen in Figure 7, which contain diacetoxymethyl ether substituents attached to the phenolic oxygens on fluorescein. The increase in fluorescence after enzyme addition can be precisely measured over time to determine how well the esterase recognizes different substrates (Lavis). The relationship between substrate concentration and the rate of the reaction can be plotted and fitted to the Michaelis-Menten equation, Equation 1 (Nelson).

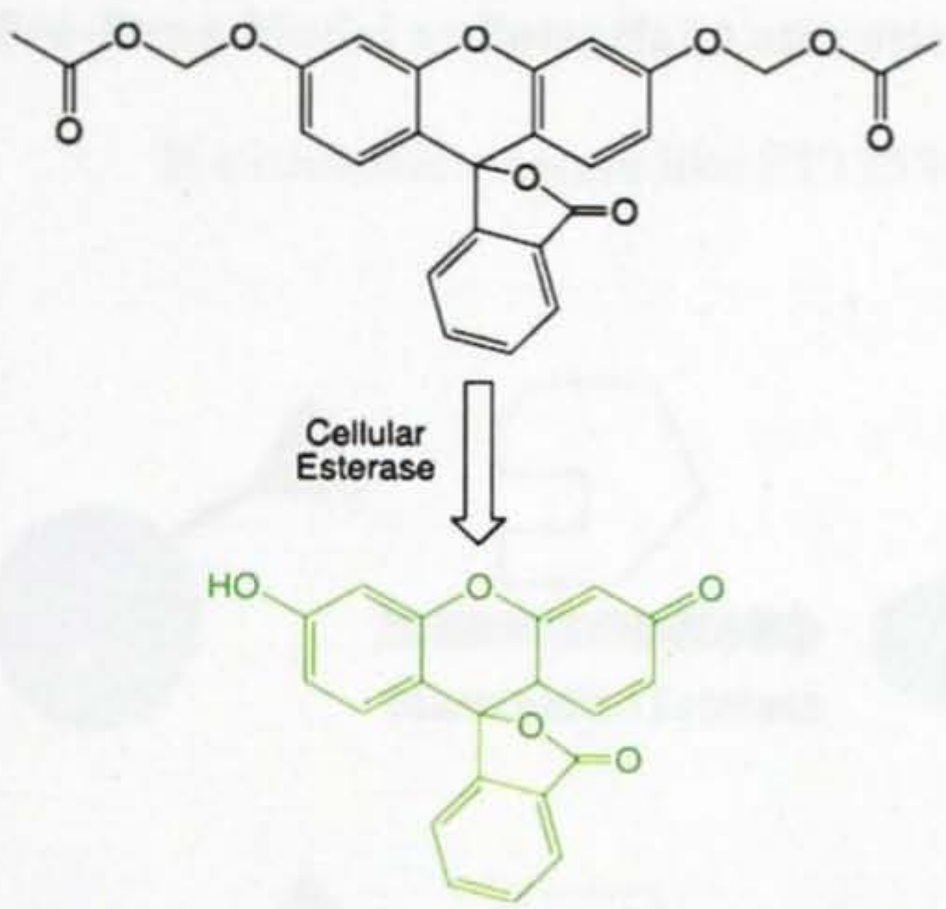

Figure 6: Schematic of ester hydrolysis of diacetoxymethyl ether fluoroscein, a latent fluorophore, by a cellular esterase. After cleavage of the ester bond the fluorophore, fluorescein, is able to fluoresce. (Lavis 2011)

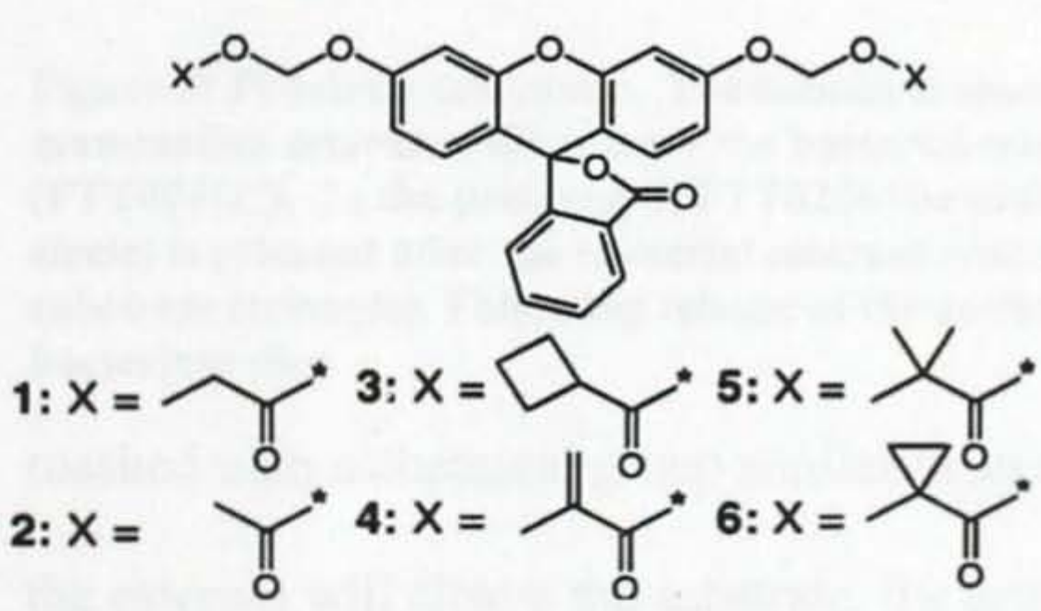

Figure 7: Latent fluorophore substrates to be tested for enzymatic activity against *F. tularensis* esterases.

Pro-Drug Model as Potential Antibiotic Treatment for Infection by *F. tularensis*

If a bacterial esterase like FTT258C shows different substrate specificity than mammalian esterases, these orthogonal substrates could be appended on common antibiotics as prodrugs, which are similar in concept to latent fluorophores. These prodrug antibiotics might serve as a valuable treatment option for infection from *F. tularensis* (Liederer). In the basic prodrug design, an antibiotic would be masked with a chemical group similar to an esterase substrate. In the bacterial cell where the esterase will cleave the substrate, the drug is therapeutically active, but in uninfected human cells, the drug would remain inactive. Ester based pro-drugs are commonly used to improve a drug's ability to be absorbed orally (Liederer). Common examples of ester-based prodrugs are statins, used for cholesterol reduction, beta blockers, for reduced blood pressure, and some medicinal steroids (Liederer).

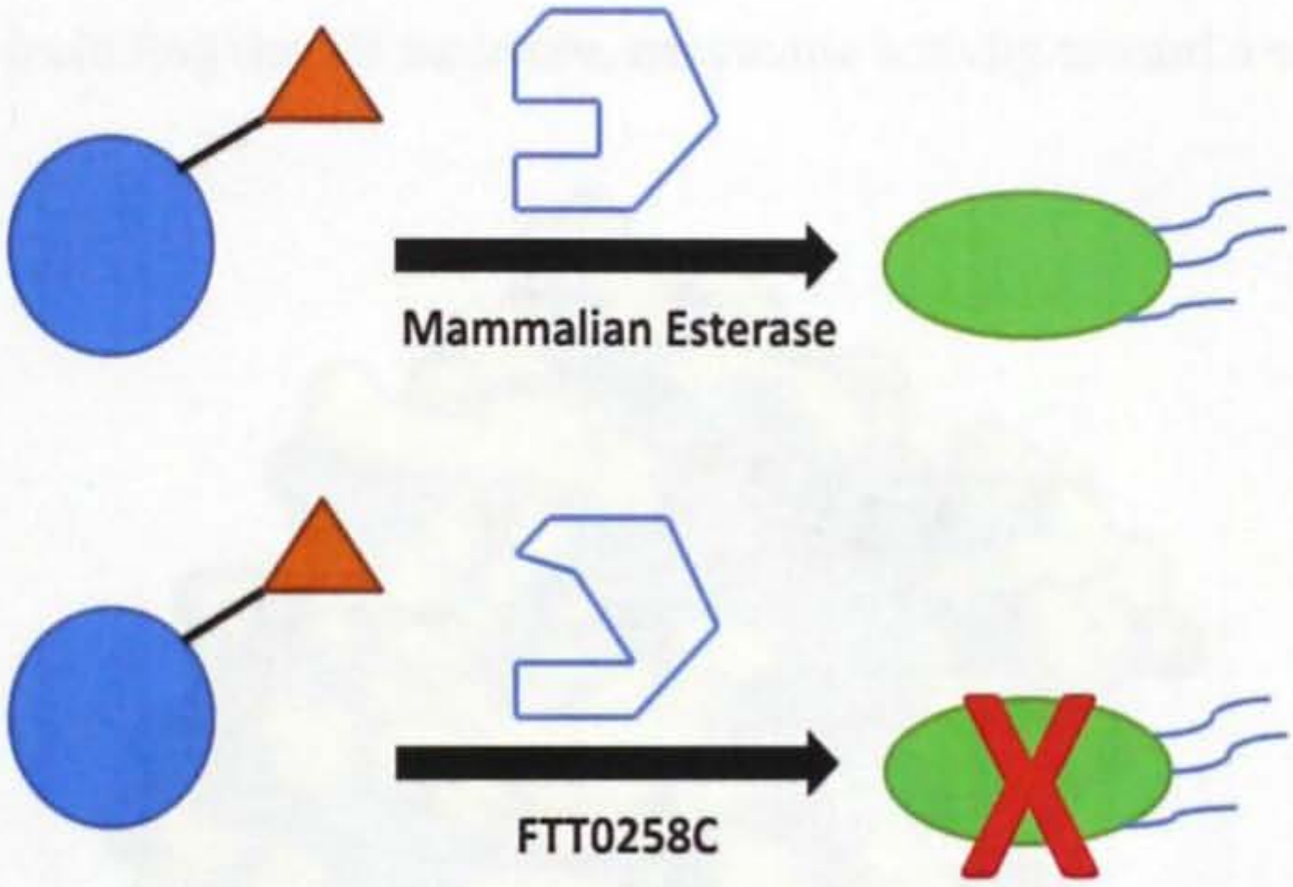

Figure 8: Pro-drug schematic. The substrate specificity of the mammalian esterase differs from the bacterial esterase (FTT0258C). In the presence of FTT0258 the antibiotic (blue circle) is released after the bacterial esterase reacts with its substrate (triangle). Following release of the antibiotic the bacterium dies.

Results and Discussion

Three Dimensional (3D) Structural Analysis

To determine the precise substrate specificity and potential biological activity of FTT0258C from *F. tularensis*, many different biochemical aspects were analyzed including the 3D structure, enzymatic activity toward a variety of substrates, and sequence alignment to other esterases. An exact 3D structure of FTT0258C is not known, but based on sequence identity between FTT0258C and human APT1 (PDB 1FJ2) a 3D model for FTT0258C was built using Swiss-Model (Devedjiev). The structural model for FTT0258C is shown in Figure 9. Figure 9 highlights the binding pocket of FTT0258C and shows that this pocket is quite large, deep, and open, potentially allowing the enzyme to accommodate many diverse substrates. Pesaresi and Lamba (2010) observed a similar long trough in the structure of the homologous carboxylesterases, PA3859, from *P. aeruginosa* and they proposed that this long, shallow binding pocket allowed this bacterial esterase to effectively bind and catalyze the hydrolysis of various short acyl chains.

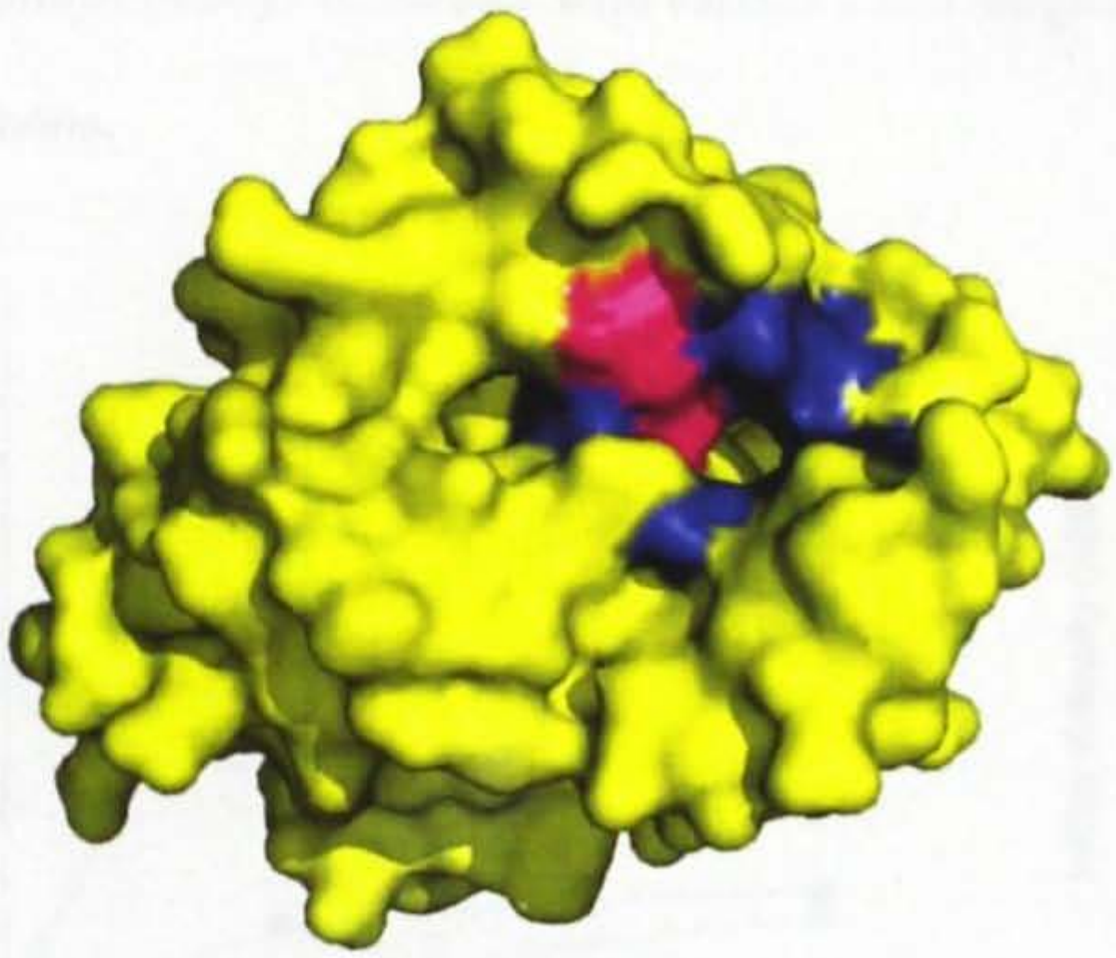

Figure 9: Overall structure and binding pocket of FTT0258C from *F. tularensis*. Two residues from the catalytic triad, Ser116 and His202 are highlighted in pink. Amino acid residues highlighted in blue were mutated to alanine for the characterization of FTT0258C.

Kinetic Analysis with Latent Fluorophores

Measurement of the precise kinetic activity of FTT0258C was used to provide more evidence about the proper substrate specificity and physiological role of the esterase. The kinetic activity and substrate specificity were determined by reacting purified FTT0258C with the latent fluorophore substrates showcased in Figure 7, as well as p-nitrophenyl substrates with carbon chain lengths varying from two to twelve carbons.

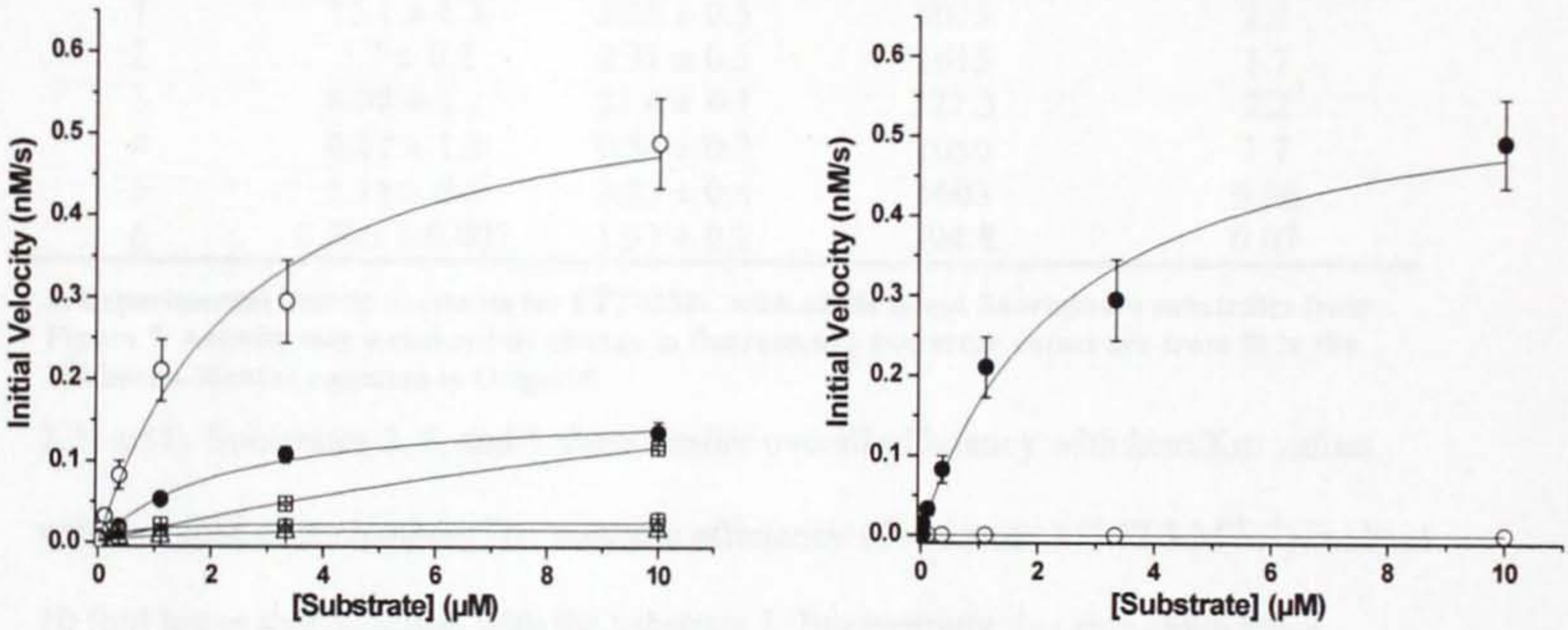

Figure 10[a]: Michaelis-Menten plot for wild type FTT0258C and knock out, S116A, mutant with six different latent fluorophore substrates. (Left) Michaelis-Menten plot for FTT0258C with all six latent fluorophore substrates: Ope circle (1), Closed Circle (3), Open Square (5), Open Diamond (2), Closed Square (6),Open Triangle (4) Right: Michaelis-Menten Plot for FTT0258C and mutant S116A with Substrate 1: Closed Circle (WT), Open Circle (S116A). Numbering refers to substrate number from Figure 1. a) Error values are the standard error for triplicat kinetic experiments.

The Michaelis-Menten plots (Figure 10) and kinetic constants represented in Table 1 show that FTT0258C was able to cleave all of the various side chains of the latent fluorophores. Activity with substrate 1 (5075 $M^{-1}s^{-1}$) is approximately three times more efficient than the next most active which is substrate 2 (1615 $M^{-1}s^{-1}$). Substrate 1 is a fairly simple esterase substrate with only a propyl sidechain, but the K_m value (2.58

μM) for substrate 1 is not the lowest amongst the six substrates, suggesting preferential binding of longer carbon chains.

The second most active enzyme catalyzed reaction occurs with substrate 2, an acetyl side chain. For such a simple substrate, the turnover ($3.7x10^{-3}$ s^{-1}) is not significantly increased (3 fold slower), but binding affinity is similar to substrate 1 (K_m 2.31 μM). Substrates 2, 4, and 5 show similar overall efficiency with kcat/Km values within 1-fold of each other. The catalytic efficiency of substrate 3 (377.3 $M^{-1}s^{-1}$) is about 10 fold lower than reaction with the substrate 1. Interestingly this side chain has a cyclobutyl group, and catalytic turnover for the substrate is the second highest of all the substrates. However, a 10-fold increase in K_m (21.4 μM) results in the decreased overall efficiency compared to Substrate 1. Substrate 4, which has an α,β unsaturated bond for its side chain, has the lowest K_m value (0.54 μM). The K_m value is 4 times lower with this substrate than the most efficient enzyme catalyzed reaction which indicates tighter binding. However, turnover rate ($0.57x10^{-3}$ s^{-1}) with substrate 4 is decreased 200 fold.

Table 1: Kinetic Values for Latent Fluorophore Hydrolysis by FTT0258C[a]

	Wild-type			*S116A*
Substrate #	k_{cat} (10^{-3} s^{-1})	K_m (μM)	k_{cat}/K_m ($M^{-1}s^{-1}$)	k_{cat}/K_m ($M^{-1}s^{-1}$)
1	13.1 ± 1.3	2.58 ± 0.5	5075	2.1
2	3.7 ± 0.2	2.31 ± 0.3	1615	1.7
3	8.08 ± 1.1	21.4 ± 4.1	377.3	2.2
4	0.57 ± 1.5	0.54 ± 0.2	1050	1.7
5	5.18 ± 0.5	3.23 ± 0.8	1603	0.56
6	0.395 ± 0.001	1.33 ± 0.2	294.8	0.07

a. Experimental kinetic constants for FTT0258C with all six latent fluorophore substrates from Figure 7. Activity was measured by change in fluorescence and error values are from fit to the Michaelis-Menten equation in Origin™.

For the two substrates with tertiary carbons, the activity drops slightly from substrate 1 (k_{cat}/K_m = 1603 $M^{-1}s^{-1}$ for substrate 5 and 294.8 $M^{-1}s^{-1}$ for substrate 6). The

steric hindrance of these two ester bonds with tertiary carbons alpha to the carbonyl make them difficult to hydrolyze. However, the K_m value (1.33 μM) for substrate 6 is slightly lower than substrate 1, but the turnover (0.395 x10^{-3} s^{-}1) is decreased 30 fold. This slow kinetic hydrolysis rate of substrate 1 by wild-type FTT0258C matches the low background hydrolysis rate measured with the S116A mutant.

The FTT0258C mutant, S116A, has the nucleophilic serine residue mutated to an inactive alanine residue, which makes the enzyme catalytically inactive. Hydrolysis of the latent fluorophore substrates by the S116A serves as a measurement of background hydrolysis. For substrate 1, the S116A mutant is nearly 2500 times less active (k_{cat}/K_m = 2.1 $M^{-1}s^{-1}$) and shows that the measured fluorescent signal is caused by the hydrolysis of the substrates by FTT0258C. The low kinetic constant values for S116A show that background hydrolysis of the latent fluorophore substrates is minimal and indicates the extreme stability of the tertiary carbon substrates. The low background hydrolysis rate highlights the incredible value of latent fluorophores for use as esterase substrates.

Kinetic Analysis with p-Nitrophenyl Substrates

To better compare the activity of FTT0258C with bacterial carboxylesterases, kinetic reactions were performed with four common p-nitrophenyl (p-NP) esterase substrates (Pesaresi and Kim)

Table 2: Kinetic Values for p-Nitrophenyl Substrate Hydrolysis by FTT0258C (a)

Substrate Chain Length	k_{cat} (10^{-3} s^{-1})	K_m (mM)	k_{cat}/K_m ($M^{-1}s^{-1}$)
2	5.84 ± 0.3	1.9 ± 0.3	3048.6
4	3.41 ± 0.3	0.79 ± 0.2	4283.18
8	0.314 ± 0.07	0.072 ± 0.04	4765.4
12	0.128 ± 0.07	2.36 ± 1.7	54.188

a: Experimental kinetic constants for FTT0258C with p-nitrophenyl (NP) substrates with carbon chain lengths of 2, 4, 8, and 12 carbons. Activity was measured by change in absorbance over time at 410nm.

(Table 2).

The overall enzymatic efficiency of FTT0258C is very similar for carbon chain lengths of two, four, and eight. In a similar pattern to the activity with C2 and C3 chain lengths of the latent fluorophores, the p-NP C2 and C4 substrates show that the longer carbon chain has improved binding affinity but decreased turnover. In a general comparison to the latent fluorophore substrates, the K_m values for the NP substrates increased, but turnover numbers (k_{cat}) also increased slightly. Considering the twelve and eight carbon chain lengths, substrate activity with the shorter chain is about 90 times more efficient than the twelve carbon substrate. This significant decrease in activity is somewhat surprising considering the role that the homologous APT1 esterases have removing fatty acid chains from other proteins. However, a similar drop in activity for carbon chain lengths longer of twelve and longer has been reported for the *P. aeruginosa* carboxylesterase (Pesaresi 2005 "Insights"). Pesaresi attributes some of the decreased activity to complications with solubility of these substrates in water. The carboxylesterase from *P. fluorescens* is reported to react with p-NP substrate chains of two through ten carbons (Kim). These similarities provide additional evidence that FTT0258C belongs to the bacterial carboxylesterase family, as it prefers shorter carbon chain lengths of less than 10 carbons.

Binding Pocket Mutation Investigation

In addition to characterizing wild type FTT0258C, five different single amino acid mutants of FTT0258C were expressed, purified, and reacted with two of the latent fluorophore substrates. In addition to characterization with latent fluorophores, thermal stability of the mutants was investigated (Figure 14), and an amino acid sequence

alignment was generated that compared the primary structure of FTT0258C to similar carboxylesterases from multiple organisms (Table 3). This set of experiments was used to try to understand more about the binding pocket of FTT0258C (Figure 11).

Amino acid residues for mutation were selected based on their proximity to the catalytic serine residue, Ser 116. Selected amino acids for mutations were L22A, I57A, L72A, F115A, and V172A and all of these amino acids are large hydrophobic amino acid. These amino acids for mutation were not selected based on their hydrophobicity, but rather on their location in relationship to the catalytic triad. Mutation studies were also used to determine if the structural model for FTT0258C, based on human APT1 (Devedjiev), served as a good representation for the actual 3D structure of the esterase. If these five amino acids are located around the binding pocket as predicted by the structure than a significant change in catalytic activity should be observed between the mutant and wild-type enzymes.

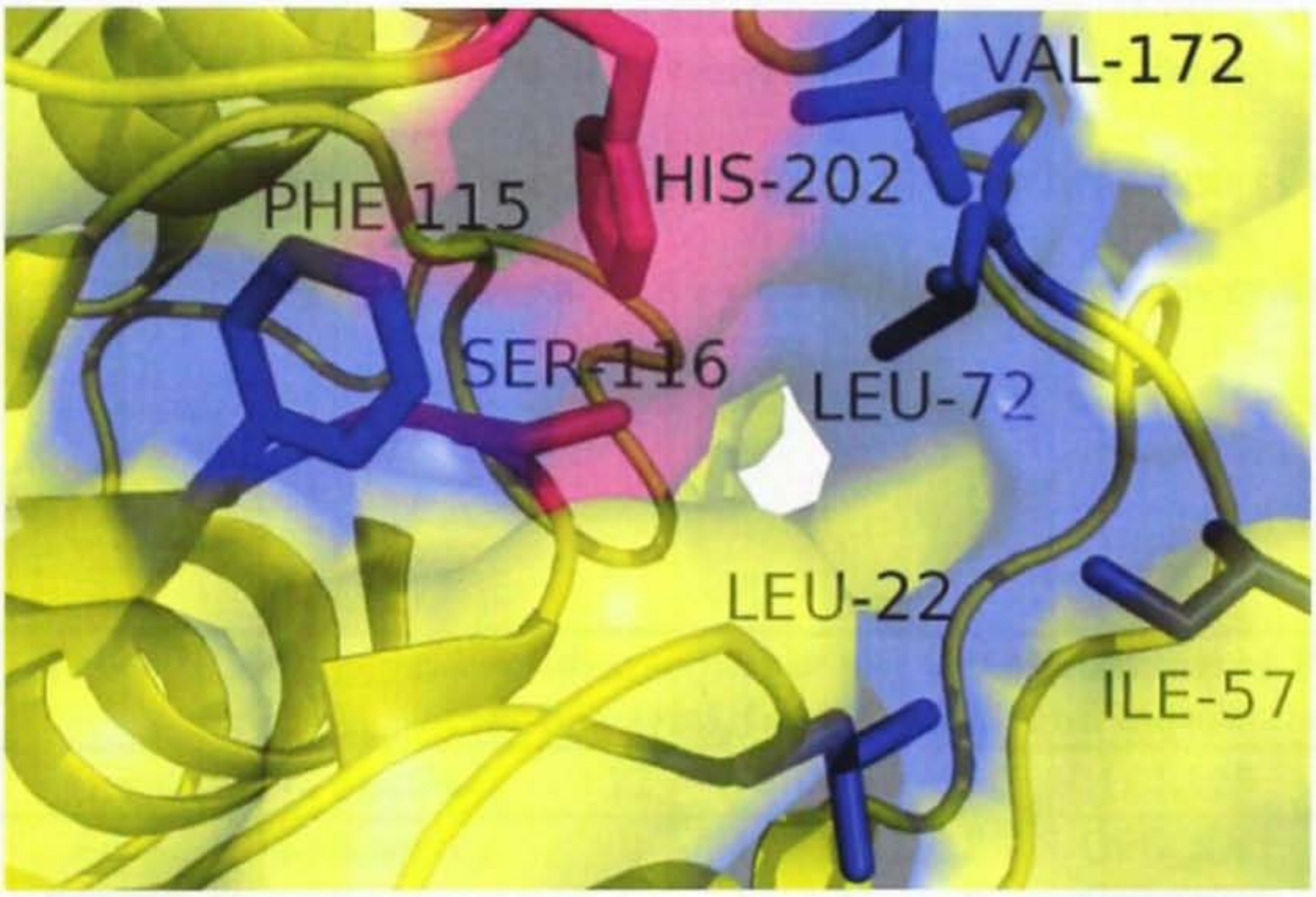

Figure 11: Close up view of the FTT0258C binding pocket and mutation locations. Pink represents the catalytic amino acids (Ser116 and His202). All residues highlighted in blue represent amino acids that were mutated to alanine for this investigation.

The mutant with the most significant decrease in activity was the L22A mutant. The kinetic activity of mutant L22A was measurable with substrate 1 (1.083 $M^{-1}s^{-1}$), but

is nearly 5000 fold decreased compared to the wild type. With substrate 5, the kinetic activity of the L22A mutant was not determinable, because the fluorescent signal was below background hydrolysis levels. The decreased activity seen with both substrates indicates that Leu22 is very important to the function and structure of the esterase. In the sequence alignment, position 22 is completely conserved as a leucine residue across all organisms and esterases. Previously, the homologous amino acids (Leu22 and Leu23) in the carboxylesterases of *P. aeruginosa* and *P. fluorescens*, respectively, were proposed based on structural location to be essential components of the oxyanion hole which provides hydrogen bonding stability during substrate hydrolysis (Pesaresi and Kim). The dramatic decrease in catalytic activity upon mutation provides evidence that Leu22 in FTT0258C likely plays a similar role in the oxyanion hole for transition state stabilization.

Table 3: Amino acid residue sequence alignment comparing FTT0258C from *F. tularensis* to other bacterial, fungal, mold, and mammalian esterases.

Organism (Function)	22	57	72	115	114-120	172	% Identity
Francisella tularensis	L	I	L	F	GFSQGG	V	100
Francisella philomiragia	L	I	L	F	GFSQGG	V	90
Marinobacter aquaeolei	L	I	M	F	GFSQGG	I	42
Shewanella denitrificans	L	I	L	F	GFSQGG	V	41
Bovine (APT1)	L	L	L	F	GFSQGG	L	40
Pseudomonas aeruginosa	L	V	F	F	GFSQGG	V	40
Human (ATP1)	L	L	L	F	GFSQGG	L	39
Pseudomonas fluorescens	L	I	M	F	GFSQGG	V	38
Neurospora (ATP1)	L	A	L	F	GFSQGG	V	37
Mouse (ATP2)	L	L	L	F	GFSQGG	M	35
Human (APT2)	L	L	L	F	GFSQGG	M	34
Cryptococcus (APT1)	L	L	L	F	GFSQGG	V	33
Slime Mold (ATP1)	L	L	L	F	GFSQGA	V	33
Candida glabrata (APT)	L	A	L	F	GFSQGA	V	32

Esterases were chosen based on sequence identity to FTT0258C, and are organized by decreasing percent identity. Amino acid residue alignment by location in *F. tularensis* Amino acid sequences were aligned using the standard settings in ClustalW.

The I57A mutant of FTT0258C retains the highest enzymatic activity; however, the activity (2380 and 924.6 $M^{-1}s^{-1}$) is still decreased by about half compared to the wild type. Interestingly, the I57A mutant has the highest K_m values (0.68 and 0.93 μM) of the different mutants, but the best turnover (1.6 and 0.86 10^{-3} s^{-1}), resulting in improved efficiency compared to the other mutants. Compared to the wild type FTT0258C kinetic values with substrate 5, the I57A mutant is 100-fold less active with respect to overall

Table 4: Kinetic Values for Latent Fluorophore Hydrolysis by FTT258C Mutants: Substrate 1

Enzyme	k_{cat} (10^{-3} s^{-1})	K_m (μM)	k_{cat}/K_m (M^{-1} s^{-1})
Wild Type	13.07 ± 1.3	2.58 ± 0.5	5074.62
L22A	0.0013 ± 0.00003	1.21 ± 0.09	1.083
I57A	1.6 ± 0.04	0.68 ± 0.07	2380.7
L72A	0.018 ± 0.0004	0.52 ± 0.05	35.177
F115	0.0085 ± 0.0004	0.44 ± 0.09	19.2
V172A	0.022 ± 0.0007	0.058 ± 0.07	38.617

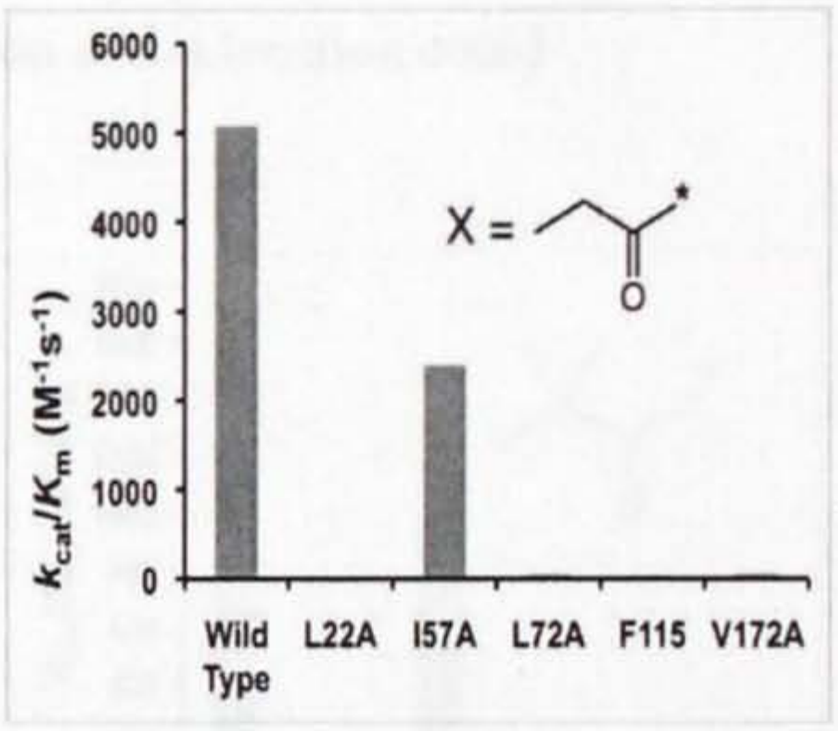

Figure 12: (Right) Kinetic efficiency (k_{cat}/K_m) for FTT0258C and mutants when reacted with latent fluorophore substrate 1.

efficiency. The near wild-type activity of the I57A mutant can be explained by its relative location within FTT0258C, where Ile57 is the farthest mutation location from the catalytic triad residues. Additionally, an isoleucine at position 57 is not as well conserved as the other binding pocket residues and two species (*Neurospora* and *Candida glabrata*) even have alanine at the analogous position, suggesting that a more disruptive substitution might be necessary to further investigate the role of position 57 in the catalytic activity of FTT0258C.

The L72A mutant is nearly 150 times less efficient (35.18 $M^{-1}s^{-1}$) than the wild type esterase with substrate 1 and 100 fold less efficient with substrate 5 (15.86 $M^{-1}s^{-1}$).

Leu72 is located in close proximity to Ser116 and His202, which are two members of the catalytic triad. Structural changes to this location could alter the overall shape of this portion of the binding pocket. The leucine residue at position 72 is conserved across most organisms and functions, which suggests it is quite important to the structure and/or function of esterases in this class. The conservation across multiple organisms suggests an evolutionary selective pressure for Leu at this position and can explain the significantly decreased activity of this mutant with the latent fluorophores.

Phenylalanine 115 is located immediately adjacent to the catalytic serine, Ser116. As such, it is conserved across all organisms. Any mutation at this location could

Table 5: Kinetic Values for Latent Fluorophore Hydrolysis by FTT258C Mutants: Substrate 5

Enzyme	k_{cat} (10^{-3} s^{-1})	K_m (μM)	k_{cat}/K_m (M^{-1} s^{-1})
Wild Type	5.2 ± 0.5	3.23 ± 0.8	1603
L22A	ND	ND	ND
I57A	0.86 ± 0.03	0.93 ± 0.1	924.6
L72A	0.014 ± 0.001	0.90 ± 0.3	15.86
F115	0.00037 ± 0.00008	0.35 ± 0.01	1.057
V172A	0.0012 ± 0.0004	0.71 ± 0.3	1.648

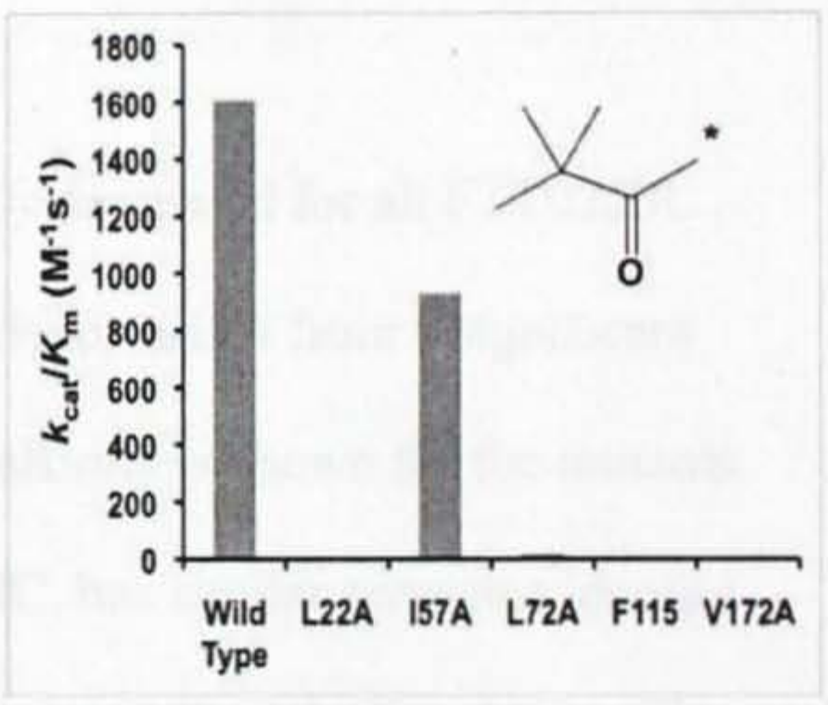

Figure 13: (Right) Kinetic efficiency (k_{cat}/K_m) for FTT0258C and mutants when reacted with latent fluorophore substrate 5. A value is not presented for L22A with substrate 5 because measurements were indiscernible from the background signal.

potentially cause problems for the stability and structure of the esterase. In fact the kinetic studies with this mutant, activity is significantly decreased compared to the wild type (19.2 and 1.057 $M^{-1}s^{-1}$). Turnover for F115A is dramatically decreased for substrate 1 (0.0085 10^{-3} s^{-1}) with the wild type being 1500 fold faster at performing the hydrolysis than this mutant. Overall the wild type is over 250 times more efficient than F115A. For substrate 5 efficiency, the wild type esterase is over 1500 fold better than F115A. The

decreased activity seen makes sense due to the proximity of this residue to the catalytic Ser and the conservation of this residue across multiple organisms.

The wild type esterase has shown to be over 100 fold more efficient at performing esterase activity than mutant V172A (38.62 and 1.648 $M^{-1}s^{-1}$). When reacted with substrate 5 this mutant is nearly 1000 fold less active than the wild type. The valine residue at position 172 represents the site of least conservation between of all the mutation locations. Conservation cannot explain the decreased activity of the mutant; however, this residue is positioned immediately adjacent to His202 which is a member of the catalytic triad. Structural changes, such as the mutation to alanine, at this location could alter the overall shape of this portion of the binding pocket thus causing the decreased kinetic activity.

In summary, the catalytic efficiency is significantly decreased for all FTT0258C mutants with both substrates. This overall decreased efficiency arises from a significant decrease in turnover, but interestingly improved binding affinity is shown for the mutants with both substrates. The *F. tularensis* esterase, FTT0258C, has similar sequence identity to human APT1 as the reported carboxylesterases from Pesaresi "Insights" and Kim. The sequence similarity of these esterases to human APT1 provides genetic evidence that FTT0258C should be classified as a carboxylesterase. Kinetic experiments with p-NP substrates were not performed with these mutants because of their general inactivity. The significant decrease in activity of all of these mutants led to the hypothesis that these mutations were causing improper folding of the esterases. Therefore a melting temperature analysis was performed to check the mutant stability compared to wild-type FTT0258C (Table 6).

Table 6: Experimental Melting Point (°C) for FTT0258C and Mutants[a]

Wild Type	S116A	L22A	I57A	L72A	F115A	V172A
50.5 ± 0.5	51.5 ± 0.5	49.0 ± 0.5	48.0 ± 0	51.0 ± 0	39.0 ± 0	40.5 ± 0.5

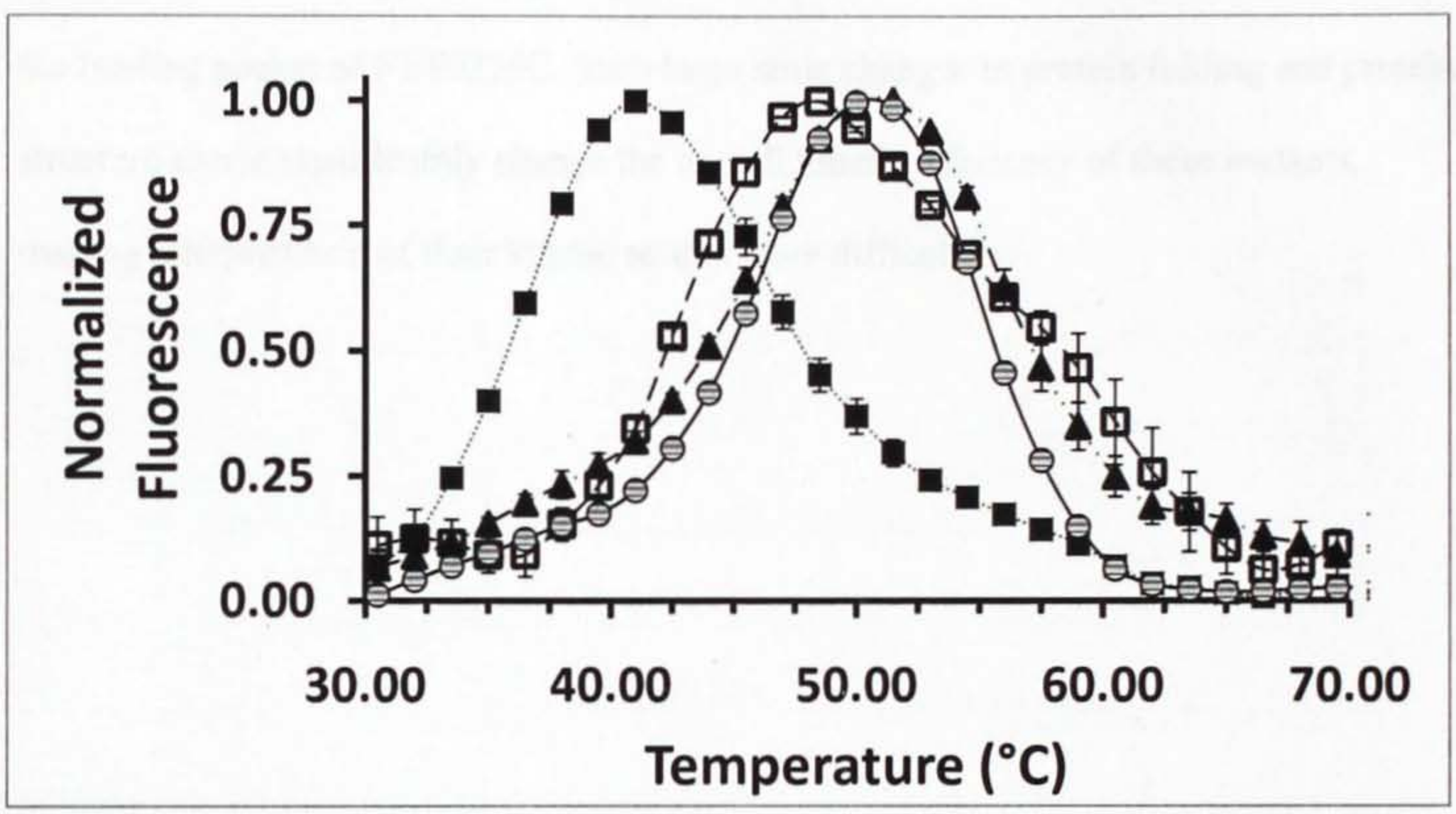

Figure 14: Thermal denaturation of FTT0258C and variants of FTT0258C. Normalized fluorescence of SyproRuby dye with increasing temperature for Wild Type FTT0258C (striped circle), I57A (open square), L72A (triangle), and V172A (closed square) mutants. Other mutant esterases are not included for clarity of the melting temperature curves.

a) The inflection point was used to determine the melting temperature (T_m) for mutant and FTT0258CC.

The melting temperature (T_m) for FTT0258C is 50.5°C (Figure 6), which is comparable to other esterases (Pesaresi and Kim). The previously referenced carboxylesterase from *P. aeruginosa* is reported to have a T_m of 55°C, which is similar to the experimental value for FTT0258C (Pesaresi 2005 "Isolation"). This similarity in stability is further evidence supporting that the studied esterase belongs to the same carboxylesterase family.

All mutants, with the exception of F115A and V172A, have similar T_m values with the greatest difference being 2.5°C lower for mutant L22A. The similarity in values

suggests that these mutants are folded correctly and the decrease in catalytic activity arises from direct contributions to the catalytic activity and not indirectly to the activity based on protein folding. The T_m values for F115A and V172A are decidedly lower than the other esterases, suggesting an important structural role for these two amino acids in the binding pocket of FTT0258C. Such large scale changes in protein folding and protein structure would significantly change the overall kinetic efficiency of these mutants, making interpretation of their kinetic results more difficult.

Conclusions

The purpose of this study was to determine the substrate specificity, kinetic activity, and likely biological function of FTT0258C from *F. tularensis*, the causative agent of tularemia. Studies performed included 3D structural analysis, primary structure comparisons, kinetic activity studies with two different types of substrates, and thermal denaturation measurements.

Overall, FTT0258C is able to perform ester hydrolysis with various short carbon chains (< 8 carbons) and simple tertiary carbon substrates. The general promiscuity of this esterase and its increased activity toward shorter carbon chain substrates suggests that it is a carboxylesterase. While the specific physiological role of similar bacterial carboxylesterases remains unknown, their amino acid sequences are highly conserved and studies such as these provide insight into the potential biological roles these enzymes could serve. Primary structure similarity of this esterase and other carboxylesterases with APT1 from multiple organisms provides evidence that this family of carboxylesterases could play a role in the removal of fatty acid chains from acylated proteins, but the substrate specificity differs from similar human enzymes.

In the future, FTT0258C and the Ser 116 mutant will be transfected into HEK293 cells and activity with latent fluorophore substrates will be measured and compared to cells without FTT0258C. These studies will provide an insight into the difference in substrate specificity of general human esterases and FTT0258C. Any difference could be utilized to develop a disease specific pro-drug model for the treatment of tularemia. Additionally, as the library of available latent fluorophores continues to expand FTT0258C will be reacted with the new substrates to gather more information about the broad substrate specificity of this carboxylesterase.

Materials and Methods

Materials

Chemical reagents purchased for these studies were obtained from Sigma-Aldrich including the p-NP substrates. All latent fluorophore substrates were generous gift of Dr. Luke Lavis from HHMI-Janelia Farm Research Campus. All phosphate buffered saline (PBS) solution used in this investigation was at pH 7.4 and comprised of the following components per liter: 8 g NaCl, 0.2 g KCl, 1.44 g Na_2HPO_4, 0.27 g KH_2PO_4, and deionized water.

Site-Directed Mutagenesis

The single amino acid mutations began with five QuikChange site directed mutagenesis reactions. To perform the QuikChange reaction, a plasmid containing the *F. tularensis* gene was annealed with DNA primers which code for the desired nucleic acid mutations. All components of the QuikChange reactions are shown in Table 7. The final ingredient, *Pfu*Turbo DNA Polymerase was added immediately before the reactions were placed in a PCR machine. The reactions were run overnight. For removing template DNA from mutated DNA, QuikChange reactions were treated with DpnI. Template DNA was digested with DpnI (1 µL) at 37°C for one hour.

Component	Concentration	Volume Used
Reaction Buffer	10x	5µL
FTT0258CDNA Primer	50 ng/µL	2µL
Oligonucleotide Primer 1	125 ng/µL	1µL
Oligonucleotide Primer 2	125 ng/µL	1µL
dNTP Mix	10mM	1µL
Deionized Water	N/A	39µL
*Pfu*Turbo DNA Polymerase	N/A	1µL

Table 7: Chemical components of the QuikChange site directed mutagenesis reactions.

Bacterial Transformation

A small amount (1 μL) of wild-type FTT plasmid or mutant plasmid DNA was added to DH5α *E. coli* cells. The mixture was put on ice to equilibrate for 15 min. The cell mixture was then exposed to a 42°C water bath for 40 s and put back on ice for 2 min and then LB solution (1 mL) was added. The bacterial cultures were placed in an incubated (37°C) shaker for approximately one hour. A portion of the cells were then applied to LB-ampicillin agar gel plates and the plates were incubated (37°C) overnight.

DNA Purification Using the Qiagen MiniPrep Protocol

Bacterial colonies were chosen from each by picking them off the agar plate with a toothpick. Each colony was placed in LB (5 mL) containing ampicillin (0.2 mg/ml). The cultures were then placed in an incubated (37°) shaker to grow overnight. A small volume (2 mL) from each bacteria culture was removed and centrifuged. The supernatant was removed and the bacterial pellet was re-suspended buffer P1 (250 μL) using a Vortexer. Buffer P2 (250 μL) was added, and the mixture was inverted to lyse the bacterial cells. After addition of the N3 buffer (350 μL), the solution was mixed immediately. The sample was then centrifuged so the solid cell material would form a pellet at the bottom of the centrifuge tube. Supernatant was then removed from the pellet and added to a QIAprep spin column. The column and supernatant were then centrifuged at about 16,000xg for approximately one minute and the flow through was discarded. Wash buffer, Buffer PE (0.75 mL), was added to the column and the sample sets were centrifuged. Flow through was discarded and then the column was spun again to remove any residual wash buffer. Elution of the DNA from the column was accomplished by the addition of deionized water (50 μL) to the column. The column was then left for

approximately 5 minutes before being centrifuged. The eluted plasmid DNA was then analyzed by sequencing and concentration measurement.

DNA Concentration Determination

A blank sample was analyzed of deionized water to serve as a zero absorbance marker. Analysis was performed using a Cary 50 spectrophotometer and absorbance data at 260nm was collected. The DNA concentration was calculated using the experimental absorbance value and Beer's law (ε=50 ng/μL as determined using Expasy ProtParam (Gasteiger)).

DNA Sequencing

Sequencing was performed off campus, but samples were prepared at Butler University. Small amounts of purified recombinant plasmid DNA were loaded into well plates and strip tubes before being sent for sequencing. All sequences were generated by GeneWiz.

Bacterial Transformation and Protein Expression

To express the proteins, the FTT or mutant plasmid was transformed into *E. coli*. An aliquot of FTT plasmid (1 μL) was added to BL21 (DE3) RIPL *E. coli*. The mixture was put on ice to equilibrate for 15 min. The cell mixture was then exposed to a 42°C water bath for 40 sec and put back on ice for 2 min. LB solution (1 mL) was added and the cells were placed in an incubated (37°C) shaker for approximately one hour. Following incubation, a small volume of transformed cells (30 μL) along with LB (70 μL) were spread onto to LB-Ampicillin (200 μg/mL)-chloramphenicol-(30 μg/mL) agar plates, and the plates were incubated (37°C) overnight.

Liquid LB cultures (5 mL) of BL21 (DE3) *E. coli* containing the FTT esterase or mutants were prepared and grown over night (37°C, 225 rpm). The saturated overnight culture (5 mL) was transferred to a larger LB flask (1000 mL) containing ampicillin and chloramphenicol. The cultures were grown until the OD_{600} was above 1.0 and protein expression induced using isopropyl-beta-D-thiogalactopyranoside (IPTG) (0.5 mM). After induction, the cultures were grown for 3 hours at 37°C and the bacterial culture pellet was collected by centrifugation for 10 minutes at 6,000xg at 4°C. The supernatant was removed, and the bacterial pellet was re-suspended in PBS buffer (5 mL). The cell solution was then stored at -20°C.

Cell Lysis

Lysozyme (50 mg) and Novagen® BugBuster 10X Protein Extraction Reagent (800 μL) was added to the bacterial cell pellet solution, mixed by inversion, and placed on an orbital shaker for 60 minutes at room temperature. The bacterial culture was centrifuged for 10 minutes at 16,000xg. Supernatant was further purified by column chromatography.

Affinity Column Chromatography

QiagenNi-NTA agarose solution (750 μL) was added to the supernatant from the bacterial cultures and allowed to equilibrate for approximately 5 minutes on an orbital shaker. This solution was then poured into a gravity-flow purification column. Column flowthrough was stored for SDS-PAGE analysis. The column was washed three times with PBS (50 mL) containing 10 mM, 25 mM, and finally 50 mM imidazole. Wash flowthrough was also saved for SDS-PAGE analysis. A PBS solution containing 250mM imidazole (600 μL) was used to elute the FTT or mutant protein from the nickel-NTA

resin. The entire volume of eluate (~600 μL) was injected into a dialysis cassette (10 kD molecular weight cut-off). The eluate was stored in the cassette in PBS at 4°C for a week before SDS-PAGE analysis.

SDS-PAGE

To determine the success of the purification, FTT samples from throughout the purifications were analyzed by SDS-PAGE. Flowthrough and wash samples (30 μL) were combined with SDS loading dye (10 μL, 4x). To prepare the purified the FTT sample, the entire volume (~600 μL) from the dialysis cassette was removed and the pure FTT (15 μL) was combined with loading dye (10 μL, 4x). All samples containing the SDS loading dye were placed in a heat block (100°C) for 10 minutes to denature the proteins.

The gels were run for approximately 45 minutes at 150V, until the dye had reached the bottom of the gel. Colloidal coomassie brilliant blue stain was added to the gel and left overnight on an orbital shaker to stain. Water was added to destain the gel and the gel was left with the water on a shaker to destain for a few days until an image could be taken for analysis.

Protein Concentration Determination

Absorbance values from a Cary 50 UV/Vis spectrophotometer were recorded at 280nm with dialysis buffer serving as a blank. From the absorbance values for each mutant and the extinction coefficient (29910 $M^{-1}cm^{-1}$) found on ExPasy (Gasteiger), the concentration of FTT0258C protein was calculated using Beer's law.

Thermal Stability Analysis

Thermal stability analysis was conducted to determine the melting point of the wild-type and mutant esterases. FTT0258C wild type and all mutants (0.5 μg/mL) were

individually combined with Sypro Ruby (1μL) and PBS to a total volume of 25 μL. Excitation and emission of the dye was measured as temperature was increased by 1.5 °C per minute from 20 to 83 °C.

Enzymatic Analysis (Lavis 2011)

Purified FTT0258C and mutants were diluted to 25 μg/mL in phosphate buffered saline (PBS) plus 0.1 mg/mL bovine serum albumin (BSA) to a total desired volume. The total volume was then aliquoted evenly to be used for enzymatic characterization assays.

A dilution series was prepared using the eight wells of a column on a 96 well-PCR plate. These analyses were performed in triplicate; therefore each mutant used three lanes worth of substrate. In rows 1-7, PBS/BSA (110 μL) was added to each well. In the bottom well of each column PBS/BSA (156.25 μL) and fluorescein based substrate (8.25 μL of 200 μM) were added. To perform the dilution series, an aliquot (55 μL) from the well containing the fluorescein substrate were transferred to the well above. This was mixed by pipette and then a small amount (55 μL) of that solution was transferred up to the above well. This pattern of mixing and transferring was continued until the transfer amount (55 μL) was added to the top well of the column. This addition of substrate and subsequent dilution by 1/3 was done for each of the columns.

An aliquot (95 μL) of each dilution was added to a 96 well black microplate in columns 1-3 and 5-7. Fluorescein (100 μL) at standard concentrations was added to the microplate in column 4 and 8. The microplate was kept covered by foil at all times to avoid exposing the substrates to light. Just before analysis, wild-type FTT0258C or an FTT0258C mutant (5 μL) was added to the substrate containing wells for a final enzyme concentration of 1.25 μg/mL. Each mutant was added to the microplate and analyzed

separately to avoid lag time between additions. The plate was placed in the fluorescent plate reader and light of 485 nm was incident on the plate. Fluorescence was measured every 15 seconds for 4 minutes and the emission at 520 nm recorded. Fluorescent values were exported to Excel and the procedure was repeated for the second mutant. The entire process of enzyme analysis was repeated to analyze the activity of wild type FTT0258C with all six latent fluorophore substrates and all mutants with substrates 1 and 5.

To determine the kinetic constants for latent fluorophore hydrolysis, a standard curve was constructed for fluorescein fluorescence versus concentration and the equation of the line used to convert latent fluorophore fluorescence into concentration. A fresh fluorescence standard curve was generated for each assay. For the initial velocities of the reaction, the change in concentration of activated fluorophore versus time was plotted and the slopes of the lines at each concentration recorded. The plot of initial velocity *versus* substrate concentration was fit to the Michaelis-Menten equation (Equation 1) using the software program, Origin™. From this equation the constants V_{max} and K_m were determined. These constants were then used with the total enzyme concentration to determine values for k_{cat} and k_{cat}/ K_m. An analysis was made comparing all of these enzyme efficiency constants to determine the substrate preferences of the wild type and mutant esterases. Assays were run until error values were in an acceptable range.

Nitrophenyl Enzymatic Analysis

A dilution series was set up using a 96 well-plate in the same manner as with the latent fluorophore experiment. Four different nitrophenyl substrates were used with side chains of carbon chain lengths of 2, 4, 8, and 12 carbons. However for this analysis, ½ dilutions were made with a high concentration of 20mM substrate 2 mM for C4, C8, and

C12. Concentrations for the longer chains were decreased to improve solubility. Additionally a concentration of 1% acetonitrile was maintained throughout the substrate dilution to improve substrate solubility. Change in absorbance (410nm) was measured for 4 minutes. Using Beer's Law, absorbance data was converted to concentration of reacted substrate but the factor, ε, which is equal to 1.034 $mM^{-1}cm^{-1}$. Final enzyme concentrations were 1.25 μg/mL for C2 and 3.75 μg/mL for C4, C8, and C12.

As with the latent fluorophore substrates, active substrate concentrations were used to determine initial velocities. Initial velocity was plotted against substrate concentration and fit to the Michaelis-Menten equation using Origin™. Kinetic constants were determined and compared for the various carbon chain lengths. Due to the relative inactivity of the mutants, only the wild-type esterase was reacted with these substrates.

References

Beckstrom-Sternberg, Stephen (2007) "Complete Genomic Characterization of a Pathogenic A.11 Strain of *Francisella tularensis* Subspecies *tularensis*" *Plos one*, **9**, e947

Devedjiev, Yancho, Dauter, Zbigniew, Kuznetsov, Sergey R., Jones, Teresa L. Z., and Derewenda, Zygmunt (2000) "Crystal Structure of the Human Acyl Protein Thioesterase I from a Single X-Ray Data Set to 1.5 A", **8**, p1137-46

Gasteiger E., Hoogland C., Gattiker A., Duvaud S., Wilkins M.R., Appel R.D., Bairoch A.;*Protein Identification and Analysis Tools on the ExPasy Server;* (In) John M. Walker (ed): The Proteomics Protocols Handbook, Humana Press (2005). pp. 571-607

Holmquist, Mats (2000). "Alpha/Beta-Hydrolase Fold Enzymes: Structures, Functions, and Mechanisms." *Current Protein and Peptide Science* 1, 209-235.

Kim, Kyeong Kyu, Song, Hyun Kyu, Shin, Dong Hae, Hwang, Kwang Yeon, Choe, Senyon, Yoo, Ook Joon, Suh, Se Won (1997) "Crystal structure of carboxylesterase from Pseudomonas fluorescens, an α/β hydrolase with broad substrate specificity" *Structure*. **5**, 12

Lavis, Luke D, Chao, Tzu-Yuan, Raines, Ronald T Lavis, Luke D (2011) "Synthesis and utility of fluorogenic acetoxymethyl ethers" *Chemical Science.* 2 (3) 522-30.

Lavis, Luke D., Chao, Tzu-Yuan, and Raines, Ronald T (2008) "Bright Ideas for Chemical Biology" *ACS Chemical. Biology.* **3,** p.142-154

Liederer, Bianca M., Borchardt, Ronald T (2006) "Enzymes Involved in the Bioconversion of Ester-Based Prodrugs" *Journal of Pharmaceutical Sciences*, **95**, 6, p1177-1195.

Nelson, David L., Cox, Michael M. *Principles of Biochemistry*. New York. Lehninger

Pesaresi, Alessandro and Lamba, Doriano (2010) "Insights into the fatty acid chain length specificity of the carboxylesterase PA38959 from *Pseudomonas aeruginosa*: A combined structural, biological, and computational study" *Biochimie*, **92**, p1787-1792

Pesaresi, Alessandro and Lamba, Doriano (2005) "Isolation, Characterization, and Heterologous Expression of a Carboxylesterase of *Pseudomonas aeruginosa* PAO1" *Current Microbiology*, **50**, p102-9

Pesaresi, Alessandro and Lamba, Doriano (2005) "Crystallization, X-Ray diffraction analysis and phasing of carboxylesterase PA3859 from *Pseudomonas aeruginosa*" *Biochimica et Biophysica Acta*, **1757**, p197-201

Plasser, Felix. www.chemical-quantum-images.blogspot.com (drawn according to Karlson P et al. *Kurzes Lehrbuch der Biochemie* (1994). Georg Thieme Verlag Stuttgart.

Potter, Philip M., Wadkins, Randy M. (2006) "Carboxylesterases-Detoxifying Enzymes and Targets for Drug Therapy" *Current Medicinal Chemistry*, **13**, 9, p1045-1054.

Pohanka, M, Skladal, P. (2009) "Bacillus *anthracis, Francisella tularensis*, and *Yersinia pestis*. The Most Important Bacterial Warefare Agents" *Folia Microbiologica*, **54**, 4 p263-272.

QuickChange Site-Directed Mutagenesis Manual

Su, Jingliang, Yang, Jun, Zhao, Daimin, Kawula, Thomas H., Banas, Jeffrey A.,, Zhang, Jing-Ren (2007) "Genome-Wide Identification of *Francisella tularensis* Virulence Determinants" *Infection and Immunity*, **75**, 6, p3089-3101

The QIAExppressionist (2003)

Weiss (2007) "*In vivo* negative selection screen identifies genes required for *Francisella* virulence" *PNAS*, **104**, 14, p6037-6042

Ziedman, Ruth, Jackson, Caroline S., and Magee, Anthony I. (2009) "Protein acyl thioesterases (Review)" *Molecular Membrane Biology*, **26**, 1-2, p32-41

Acknowledgements

I would like to thank my research advisor and mentor, Dr. Jeremy Johnson for all of his guidance throughout this entire project. I would also like to acknowledge the Butler University Chemistry Department for support and materials. This work has been supported by the Holcomb Undergraduate Committee through grants for research and travel to present at a national American Chemical Society (ACS) meeting. Additional support for travel was received from a grant through the local ACS chapter. Academic support was also appreciated and received from the Honors Department at Butler University. Finally, I would like to thank Dr. Geoffrey Hoops for being my thesis reader.